Finite Elements in Analysis and Design 86 (2014) 51–60

Contents lists available at ScienceDirect

Finite Elements in Analysis and Design

journal homepage: www.elsevier.com/locate/finel

Modeling metal deposition in heat transfer analyses of additive manufacturing processes

Panagiotis Michaleris

Department of Mechanical and Nuclear Engineering, The Pennsylvania State University, Pan Computing LLC, United States

ARTICLE INFO

Article history:
Received 5 July 2013
Received in revised form
27 March 2014
Accepted 1 April 2014
Available online 28 April 2014

Keywords:
Additive manufacturing
Metal deposition
Element activation
Heat transfer

ABSTRACT

Additive Manufacturing (AM) processes for metallic parts using both laser and electron beam heat sources are becoming increasingly popular due to their potential of producing near net shape structural components. The thermal history generated by additive manufacturing is essential in determining the resulting microstructure, material properties, residual stress, and distortion.

In this work finite element techniques for modeling metal deposition heat transfer analyses of additive manufacturing are investigated in detail. In particular, both quiet and inactive element activation are reviewed in detail and techniques for minimizing errors associated with element activation errors are proposed. 1D and 3D numerical examples are used to demonstrate that both methods can give equivalent results if implemented properly. It is also shown that neglecting surface convection and radiation on the continuously evolving interface between active and inactive elements can lead to errors. A new hybrid quiet inactive metal deposition method is also proposed to accelerate computer run times.

1. Introduction

Additive Manufacturing (AM) processes for metallic parts using both laser and electron beam heat sources have the potential of producing near net shape structural components over a range of sizes (mm^3 through m^3). Applications range from customized medical implants to aerospace components. Both laser and electron beam based deposition systems have been utilized to deposit a range of materials. All Additive Manufacturing processes are similar in that a three dimensional part represented by a CAD file is sliced into layers (build plan) which in turn define scan trajectories of the heat source. A high power energy source (laser or electron beam) is used to heat and melt metal powder or wire, which solidifies to form a fully dense layer. The powder may be fed to the heat source through nozzles or may be raked into flat layers in powder bed systems. The addition of multiple layers can produce a three dimensional fully dense part.

Significant research has been devoted over the past ten years into investigating the effects of processing parameters on the resulting microstructure during additive manufacturing [1–7]. Another concern in additive manufacturing is distortion and residual stress [8–13]. The thermal history generated by additive manufacturing is essential in determining the resulting microstructure, material properties, residual stress, and distortion.

Modeling the thermal history of the additive manufacturing process is similar to modeling multi-pass welding [4,14–16]. Thermo-mechanical modeling of welding has been an active research area since the late 1970s [17–19]. A detailed review of finite element modeling for welding is available in references [20–27]. Typically, transient heat conduction analyses are performed in Lagrangian reference frames as opposed to Eulerian transport analyses which most often used to predict the temperature field and physical shape of the melt pool [28–32], buoyancy, surface tension, and magneto-hydro-dynamic effects [33], or powder melt pool interaction [34].

Building a complex part with additive manufacturing may require depositing hundreds or thousands of layers of material which compared to multi-pass welding introduces significant computational cost. Therefore, computational efficiency becomes paramount. Notable work in the thermal and microstructural modeling in additive manufacturing is available in Refs. [1–5,7]. Residual stress and deformation modeling is investigated in Refs. [14–16,35,36].

The material deposition in additive manufacturing is modeled by using inactive or quiet elements which are activated as the added material (powder or wire) solidifies. Two metal deposition methods are reported for modeling material deposition: (1) the use of *quiet* or (2) *inactive* elements [23,37,38]. In the *quiet* approach, the elements are present in the analysis but are assigned properties so they do not affect the analysis. In the *inactive* element approach, elements are not included in the analysis until the corresponding material has been added. A variety of general purpose commercial codes have been reportedly used to model metal deposition: Zhu et al. [39] use Ansys et al. [40,41] use Adina et al. [42] and Ye et al. [43] use Abaqus et al. [44] use Comsol, and Lundback and Lindgren [14] use Marc. However, the numerical approach implemented

http://dx.doi.org/10.1016/j.finel.2014.04.003
0168-874X/

during element activation and potential sources of errors or numerical efficiency are not investigated in these references. In welding, the size filler metal is usually small compared to the base metal, and errors introduced by element activation may be negligible. However, in additive manufacturing, the size of the deposited material is significantly larger and thus element activation errors could be significant.

The objective of this work is to investigate finite element techniques for modeling metal deposition in heat transfer analyses of additive manufacturing and demonstrate potential sources of error. In particular, both quiet and inactive element activation are reviewed in detail and techniques for minimizing errors associated with element activation errors are proposed. 1D and 3D numerical examples are used to demonstrate that both methods can give equivalent results if implemented properly. Is also shown that neglecting surface convection and radiation on the continuously evolving interface between active and inactive elements can lead to errors. A new hybrid quiet inactive metal deposition method is also proposed to accelerate computer run times.

2. Transient conductive heat transfer of additive manufacturing

This section provides a brief summary of the finite element formulation for transient conductive heat transfer. For more details see Ref. [45]. Heat transfer through mass transport in the melt pool is not directly simulated in this study. Its effects are introduced into the simulation by a distributed heat input model [46]. Enforcing energy balance in a Lagrangian reference frame $\mathbf{x}$ for a domain of volume V (see Fig. 1) results into the following partial differential equation:

$$Q(\mathbf{x},t)-\frac{dH}{dt}(\mathbf{x},t)-\nabla\cdot\mathbf{q}(\mathbf{x},t)=0$$

in the entire volume V of the material (1)

where $\mathbf{x}$ is spatial coordinate and t is time. T is the temperature, $\mathbf{q}$ is the heat flux vector, Q is the body heat source, and H is the enthalpy.

The initial temperature field is given by

$$T(\mathbf{x},{}^0t)={}^0T(\mathbf{x}) \quad \text{in the entire volume } V \tag{2}$$

where ${}^0T(\mathbf{x})$ is the prescribed initial temperature. The following boundary conditions are applied on the surface,

$$T(\mathbf{x},t)=T^p(\mathbf{x},t) \quad \text{on the surface } A_T \tag{3}$$

$$q^s(\mathbf{x},t)=q^p(\mathbf{x},t) \quad \text{on the surface } A_q \tag{4}$$

where $T^p(\mathbf{x},t)$ and $q^p(\mathbf{x},t)$ represent the prescribed temperature and temperature-dependent surface flux, respectively. For surface convection and radiation, $q^p(\mathbf{x},t)$ is defined as follows:

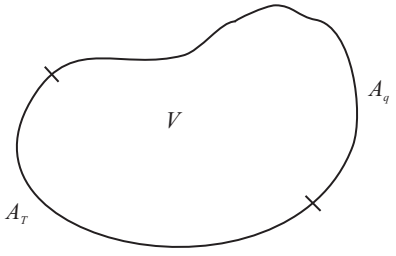

Fig. 1. A body with volume V, prescribed temperature on surface A_T, and prescribed surface flux on surface A_q.

$$q^p(\mathbf{x},t)=h\,(T-T_\infty)+\epsilon\sigma(T^4-T_\infty^4) \tag{5}$$

where, h is the convection coefficient, and T_∞ is the room temperature. ϵ is the emissivity and σ is the Stefan–Boltzmann constant.

The energy flux q is expressed as a function of temperature T using the nonlinear isotropic Fourier heat flux constitutive relation:

$$\mathbf{q}=-k(T)\nabla T \tag{6}$$

where, k is the thermal conductivity. The rate of the enthalpy can also be rewritten as

$$\frac{dH}{dt}=\frac{dH}{dT}\frac{dT}{dt}=\rho C_p\frac{dT}{dt} \tag{7}$$

where ρ is the density of the flowing body, C_p is the specific heat.

Substitution of Eqs. (6) and (7) into Eq. (1) results into the following:

$$Q(\mathbf{x},t)-\rho C_p\frac{dT}{dt}+\nabla\cdot[k(T)\nabla T]=0$$

in the entire volume V of the material (8)

Using an implicit formulation the temporal derivatives at time ${}^nt$ are approximated by the backward finite difference:

$$\frac{d^nT}{d^nt}\simeq\frac{{}^nT-{}^{n-1}T}{{}^nt-{}^{n-1}t} \tag{9}$$

where, ${}^nT$ and ${}^{n-1}T$ are the temperatures at times ${}^nt$ and ${}^{n-1}t$, respectively.

Using the Galerkin finite element discretization and the Newton–Raphson solution scheme, Eqs. (8) and (4) result into the following element residual $\mathbf{R}$ and Jacobian $d\mathbf{R}/d^n\mathbf{T}$:

$$\mathbf{R}=\int_{V_{element}}\left\{\mathbf{B}^T\mathbf{k}\mathbf{B}^n\mathbf{T}-\mathbf{N}^TQ+\mathbf{N}^T\mathbf{N}\rho C_p\frac{{}^n\mathbf{T}-{}^{n-1}\mathbf{T}}{{}^nt-{}^{n-1}t}\right\}dV+\int_{A_{q_{element}}}\mathbf{N}^Tq^p\,dA \tag{10}$$

$$\frac{d\mathbf{R}}{d^n\mathbf{T}}=\int_{V_{element}}\left[\mathbf{B}^T\mathbf{k}\mathbf{B}+\mathbf{B}^T\frac{\partial\mathbf{k}}{\partial T}\mathbf{B}^n\mathbf{T}\mathbf{N}-\mathbf{N}^T\frac{\partial Q}{\partial T}\mathbf{N}+\mathbf{N}^T\mathbf{N}\rho C_p\frac{1}{{}^nt-{}^{n-1}t}\right]dV+\int_{V_{element}}\left[\mathbf{N}^T\mathbf{N}\rho\frac{\partial C_p}{\partial T}\mathbf{N}\frac{{}^n\mathbf{T}-{}^{n-1}\mathbf{T}}{{}^nt-{}^{n-1}t}\right]dV+\int_{A_{q_{element}}}\mathbf{N}^T\frac{\partial q}{\partial T}\mathbf{N}\,dA \tag{11}$$

where, $\mathbf{T}$ is the element temperature nodal vector, and $\mathbf{N}$ and $\mathbf{B}$ are the operators that compute the temperature and temperature gradient as follows:

$$T=\mathbf{N}\mathbf{T} \tag{12}$$

$$\nabla T=\mathbf{B}\mathbf{T} \tag{13}$$

3. Material deposition modeling

Two metal deposition methods are reported in the literature for modeling material deposition: (1) the *quiet* and (2) the *inactive* element method [14,23,37,38]. In this section the methods are described in further detail.

3.1. Quiet element method

In the quiet element method, the elements representing metal deposition regions are present from the start of the analysis. However, they are assigned properties so they do not affect the